Hindawi
Advances in Civil Engineering
Volume 2020, Article ID 4628924, 1 page
https://doi.org/10.1155/2020/4628924

Retraction

Retracted: Multidimensional Fragility Analysis for a NEES Frame Structure by Integrating a New Energy Damage Index: Cumulative Plastic Strain

Advances in Civil Engineering

Received 8 June 2020; Accepted 8 June 2020; Published 30 July 2020

Advances in Civil Engineering and the authors have retracted the article titled "Multidimensional Fragility Analysis for a NEES Frame Structure by Integrating a New Energy Damage Index: Cumulative Plastic Strain" [1], due to an error identified by the authors in the seismic wave selection that leads to serious errors in the final calculation results. The Energy Damage Index: Cumulative Plastic Strain constructed in the article is therefore incorrect and the article is being retracted at the request of the authors.

References

[1] Q. Wang and Z. Wu, "Multidimensional Fragility Analysis for a NEES Frame Structure by Integrating a New Energy Damage Index: Cumulative Plastic Strain," *Advances in Civil Engineering*, vol. 2019, Article ID 7323656, 11 pages, 2019.

Hindawi
Advances in Civil Engineering
Volume 2019, Article ID 7323656, 11 pages
https://doi.org/10.1155/2019/7323656

Research Article

Multidimensional Fragility Analysis for a NEES Frame Structure by Integrating a New Energy Damage Index: Cumulative Plastic Strain

Qiang Wang[1] **and Ziyan Wu**[2]

[1]*Assistant Professor, State Key Laboratory for Geomechanics and Deep Underground Engineering and School of Mechanics and Civil Engineering, China University of Mining and Technology, Xuzhou 221008, China*
[2]*Professor, School of Mechanics, Civil Engineering and Architecture, Northwestern Polytechnical University, Xi'an 710129, China*

Correspondence should be addressed to Qiang Wang; qawang@cumt.edu.cn

Received 22 March 2019; Accepted 30 May 2019; Published 26 June 2019

Academic Editor: Constantin Chalioris

Cumulative plastic strain (CPS) damage index is proposed in this study for seismic fragility analysis by integrating the force analogy method into the energy balance equation, and CPS can be defined as the ratio of the demand of plastic dissipation energy to its capacity. The cumulative plastic strain can indicate the structural damage cumulative effect under earthquakes, which makes it especially suitable to be selected as the damage index for the structural component. Threshold values of cumulative plastic strain for different performance limit state (PLS) levels are obtained through the degree of consistency of interstory drift-based fragility curves and CPS-based fragility curves. Regarding the multidimensional fragility evaluation, CPS and the floor acceleration will be selected as the quantification indices for performance limit state of the structural component and nonstructural component, respectively. The probabilistic seismic demand model (PSDM) following multivariate logarithmic normal distribution will be developed, and taking PLS uncertainty and correlation into consideration, multidimensional PLS function is constructed to identify the structural failure domain. A full-scale 2-bay 2-story frame structure for the Network for Earthquake Engineering Simulation (NEES) project is employed as the case study structure to demonstrate the proposed theory. Nonlinear dynamic time-history analysis is carried out for the structure to obtain its maximum responses under earthquakes. Consequently, the multidimensional fragility curves can be derived on the basis of CPS. Besides, the influence of PLS threshold value, engineering demand parameter (EDP) correlation, and PLS correlation on the multidimensional fragility is investigated. Results show that (1) CPS damage index can fully consider the cumulative effect of damage under earthquakes, which makes up for the deficiency of the interstory drift damage index in this aspect, (2) the multidimensional fragility framework can deal with the PLS correlation and EDP correlation simultaneously, which will generate a more precise seismic damage assessment result, and (3) multidimensional fragility is sensitive to PLS threshold values and PLS correlation parameters.

1. Introduction

Extensive damage to engineering structures under earthquakes highlighted the vulnerability of structures to seismic excitation. For the prediction of seismic damage states and performance levels for engineering structures, performance-based earthquake engineering (PBEE) intends to quantify a border range of design scopes and damage parameters over the full range of earthquake demands [1]. In the framework of performance-based earthquake engineering, the degree of structural damage is quantified and the system performance levels are classified as different states, e.g., fully operational, life safety, and near collapse. Also, hazard levels are classified as frequent, occasional, rare, and very rare events for seismic fragility evaluation. Reasonable damage index and performance limit state should not only have clear physical meaning but also should facilitate the application for the fragility analysis in PBEE framework.

Considerable efforts have been devoted to the selection of the damage index (e.g., deformation-based damage index, energy-based damage index, etc.) for different kind of structures [2]. The interstory drift is a kind of widely used deformation-based damage index [3–5]. Kazemi et al. [6] invested the fragility of steel braced frames by incorporating new spectral shape indicators and a weighted damage index. Lv and Wang [7] proposed a decision-making method of the optimal seismic fortification level for aseismic structures based on damage performance. A seismic damage index with two linearly combined weighting parameters is established, and a simplified method is provided to calculate the damage index. Ding et al. [8] considered the damage accumulation and the strain reinforcement effect of the steel and established the damage mechanics model for the steel structure based on energy dissipation theory. The use of only one damage index such as interstory drift could be unrealistic considering that there are several parameters such as forces and responses in elements, which results in damage to the structure simultaneity. Naderpour and Mirrashid [9] investigated maximum shear capacity for reinforced concrete (RC) beam-column joints by using group method of data handling (GMDH) and adaptive neurofuzzy inference system (ANFIS). During earthquake, insufficient separation gap between adjacent buildings may cause serious damages. The best way to prevent collisions is to provide sufficiently large separation distance between structures. Khatami et al. [10] made a detailed investigation of assessing the minimum separation gap as a damage index and proposed a new equation to calculate the effective periods of inelastic building. Structural ductility is an important design parameter for the structure performance evaluation, thus ductility (e.g., ductility of rotation angle and displacement ductility) is also often selected as the damage index for fragility estimation [11, 12]. Powell and Allahabadi [13] proposed a displacement ductility damage index. On the basis of this damage index, Bassam et al. [14] performed a damage assessment of a four-span bridge structure under earthquakes and proposed a new ductility damage index for the bridge piers. Regarding energy-based damage indices, Park and Ang [15] proposed a damage index as a linear function of the ductility and the hysteretic energy demand. Teran-Gilmore et al. [16] developed a plastic energy-based damage index model for reinforced concrete structures built on soft soils, with the consideration of structural plastic demands and the degradation of the hysteretic cycle. Diaz et al. [17] developed a damage index based on a linear combination of two energy functions, i.e., the strain energy and the dissipated energy, and applied this energy-based damage index for seismic performance of low-rise steel buildings. The deformation-based damage indices, e.g., peak inelastic deformation, peak roof displacement, and interstory drift, are viewed as the simple and direct index reflecting the structural damage [18, 19]. The advantage of this damage index is that it can be used conveniently in many respects with a clear physical meaning. However, it cannot deal with the structural damage accumulation effect under earthquakes very well.

Considering the aforementioned disadvantages, in the present study, a new local damage index, i.e., cumulative plastic strain, was proposed for the structural component by using plastic dissipation energy and it can consider effects of the damage caused by repeated cycles under earthquakes. Within the framework of multidimensional fragility theory, engineering demand parameters (EDPs), respectively, for the structural and nonstructural component are selected to construct multidimensional probabilistic seismic demand model and multidimensional PLS function. Further, the sensitivity of multidimensional fragility with regard to acceleration threshold and performance limit state correlation is investigated to reveal their influence on the failure probability.

2. Research Significance

Research significance and main contribution of this study is listed as follows:

(1) In this study, a new damage index, i.e., the cumulative plastic strain, is proposed on the basis of plastic dissipation energy, which can better reflect the cumulative damage of the structure under earthquakes.

(2) The multidimensional fragility curve is derived considering cumulative plastic strain and floor acceleration as quantitative performance parameters for the structural and nonstructural components, respectively. A NEES full-scale frame structure is employed as a case study structure to illustrate the applicability of this method.

(3) The sensitivity of multidimensional fragility to PLS threshold, EDP correlation, and PLS correlation is investigated. Finally, the factors that have the greatest influence on the structural failure probability can be determined.

3. Cumulative Plastic Strain Based on Plastic Dissipation Energy

3.1. Force Analogy Method. The concept of force analogy method was firstly proposed by [20], and it was originally used to solve the problem of dynamic analysis for frame structure. The force analogy method has the advantages of high efficiency, strong stability, and broad applicability. The study will apply the force analogy method for energy analysis of frame structure, and the plastic dissipation energy for the whole structure can be expressed as the sum of the energy dissipation of all plastic hinges, which are directly associated with the structural damage.

For a structural system with n horizontal degrees of freedom, such as the frame structure with n stories, assume that each story has m rotational degrees of freedom, that is, there are m plastic hinges in each story. The horizontal displacement can be described by the following expression:

$$X(t) = X'(t) + X''(t) = \begin{Bmatrix} x_1'(t) \\ x_2'(t) \\ \vdots \\ x_n'(t) \end{Bmatrix} + \begin{Bmatrix} x_1''(t) \\ x_2''(t) \\ \vdots \\ x_n''(t) \end{Bmatrix}, \quad (1)$$

where $X(t)$ is the total displacement vector, $X'(t)$ is the elastic displacement vector, and $X''(t)$ is the plastic displacement. At the location of plastic hinge, there exist elastic bending moment and plastic rotation angle. The total bending moment and plastic turning angle can be written as

$$M(T) = M'(t) + M''(t) = \begin{Bmatrix} m_1'(t) \\ m_2'(t) \\ \vdots \\ m_m'(t) \end{Bmatrix} + \begin{Bmatrix} m_1''(t) \\ m_2''(t) \\ \vdots \\ m_m''(t) \end{Bmatrix} \Theta''(t) = \begin{Bmatrix} \theta_1'(t) \\ \theta_2'(t) \\ \vdots \\ \theta_m'(t) \end{Bmatrix}, \quad (2)$$

where $M'(t)$ is the elastic moment vector corresponding to the elastic displacement and $M''(t)$ is the plastic moment vector corresponding to the plastic displacement. Considering the equilibrium and compatibility conditions, the plastic moment and the plastic displacement can be calculated:

$$M''(t) = -\left(K'' - K'^T K^{-1} K'\right)\Theta''(t), \quad (3)$$

$$X''(t) = K^{-1} K' \Theta''(t), \quad (4)$$

where K is the overall stiffness matrix, K' is the transformation matrix between the rotation angle and the restoring force, and K'' is the transformation matrix between the rotation angle and the restoring bending moment. The elastic bending moment $M'(t)$ and the elastic displacement $X'(t)$ have the following relation:

$$M\prime(t) = K'^T X'(t). \quad (5)$$

Substituting equation (4) into equation (5), we get

$$M'(t) = K'^T X'(t) = K'^T \left[X(t) - X''(t)\right] = K'^T \left[X(t) - K^{-1} K' \Theta''(t)\right]. \quad (6)$$

Substituting equations (3) and (6) into equation (2), the control equation of the force analogy method is obtained:

$$M(t) + K''\Theta''(t) = K'^T X(t). \quad (7)$$

3.2. Energy Balance Equation under Earthquakes. The basic equation of motion for the multi-degree-of-freedom frame structural system is shown as follows [21, 22]:

$$M\ddot{x}(t) + C\dot{x}(t) + Kx'(t) = -M\ddot{g}(t), \quad (8)$$

where M is the mass matrix; C is the damping matrix; $\ddot{x}(t)$ represents the acceleration of the structure relative to the ground; $\dot{x}(t)$ is the relative speed; and $\ddot{g}(t)$ is the acceleration of the ground. The absolute displacement can be written as $y(t) = x(t) + g(t)$. Thus, equation (8) can be transferred to be

$$M\ddot{y}(t) + C\dot{x}(t) + Kx'(t) = 0. \quad (9)$$

Integrating equation (9) over the time interval $[0, t_s]$, the following equation can be obtained:

$$\int_{t=0}^{t=t_s} \ddot{y}^T M\, dy + \int_{t=0}^{t=t_s} \dot{x}^T C\, dx + \int_{t=0}^{t=t_s} x'^T K\, dx = \int_{t=0}^{t=t_s} \ddot{y}^T M\, dg. \quad (10)$$

Considering $dx = dx' + dx''$, equation (10) is simplified as

$$\int_{t=0}^{t=t_s} \ddot{y}^T M\, dy + \int_{t=0}^{t=t_s} \dot{x}^T C\, dx + \int_{t=0}^{t=t_s} x'^T K\, dx' + \int_{t=0}^{t=t_s} x'^T K\, dx'' = \int_{t=0}^{t=t_s} \ddot{y}^T M\, dg, \quad (11)$$

where IE $= \int_{t=0}^{t=t_s} \ddot{y}^T M\, dg$ is seismic input energy; IE $= \int_{t=0}^{t=t_s} \ddot{y}^T M\, dg$ is kinetic energy; DE $= \int_{t=0}^{t=t_s} \int_{t=0}^{t=t_s} \dot{x}^T C\, dx$ is damping dissipation energy; SE $= \int_{t=0}^{t=t_s} x'^T K\, dx'$ is elastic deformation energy; and PE $= \int_{t=0}^{t=t_s} x'^T K\, dx''$ is plastic dissipation energy.

Thus, energy balance equation is expressed as KE + DE + SE + PE = IE. The equation shows that a part of the seismic input energy is stored in the form of kinetic energy and elastic deformation energy and the other part is transferred into damping dissipation energy and plastic dissipation energy.

3.3. Cumulative Plastic Strain. On the basis of the plastic dissipation energy, the cumulative plastic strain is defined as the damage index for structural components. According to equations (4) and (5), the plastic dissipation energy in equation (11) can be written as

$$\int_{t=0}^{t=t_s} x'^T K\, dx'' = \int_{t=0}^{t=t_s} x'^T K\left(K^{-1} K' d\Theta''\right) = \int_{t=0}^{t=t_s} x'^T K'\, d\Theta'' = \int_{t=0}^{t=t_s} m'^T d\Theta'' = \sum_{i=1}^{m} \int_{t=0}^{t=t_s} m_i' d\theta'', \quad (12)$$

where PE $= \sum_{i=1}^{m} \int_{t=0}^{t=t_s} m_i' d\theta'' = \sum_{i=1}^{m} \mathrm{PE}_i$. PE_i is the plastic dissipation energy at the ith plastic hinge and m is the number of plastic hinges. The plastic dissipation energy is expressed as the product of elastic bending moment and plastic rotation angle.

In the study, the cumulative plastic strain is defined as the ratio of the demand of plastic dissipation energy to its capacity, which has the following form:

$$\varepsilon = \underset{i}{\mathrm{MAX}}\left[\frac{\mathrm{PE}_i}{f_y A_i d_i}\right], \tag{13}$$

where f_y is the yield stress of the component; A_i is the sectional area of the component; d_i is the length of the component; and PE_i represents the plastic dissipation energy at the plastic hinge.

4. Structural Multidimensional Fragility Analysis

4.1. Definition of Multidimensional Fragility. Seismic fragility is defined as the conditional probability that the seismic demand (or structural response) exceeds the corresponding capacity, specified for a certain performance limit state level, under given seismic intensity measures. When multiple demand parameters are considered, the traditional fragility can be extended to the multidimensional fragility:

$$P_f = P\left\{\bigcup_{i=1}^{n}\left(R_i \geq r_{\mathrm{lim},i}\right)\,\middle|\, I\right\}, \tag{14}$$

where R_i represents the seismic demand parameters (e.g., deformation, stress, and energy), $r_{\mathrm{lim},i}$ is performance limit state threshold, and I is ground motion intensity parameter, e.g., peak ground acceleration (PGA) or spectral acceleration (S_a). In this case, probabilistic seismic demand model follows multivariate logarithmic normal distribution, and its probability distribution density can be calculated by [23]

$$f(r_1, r_2, \ldots, r_n) = \frac{1}{(2\pi)^{n/2}|\Sigma|^{1/2}(r_1, r_2, \ldots, r_n)} \cdot \exp\left\{-\frac{1}{2}(\ln r - \mu)^T \Sigma^{-1}(\ln r - \mu)\right\}, \tag{15}$$

where $\ln r = [\ln r_1,\ \ln r_2, \ldots,\ \ln r_n]^{\mathrm{T}}$; $\sum$ is the mean vector of $Y = [\ln R_1,\ \ln R_2, \ldots, \ln R_n]^{\mathrm{T}}$; and $\sum$ is the covariance matrix of Y, which represents the correlation between different seismic demand parameters.

4.2. Multidimensional Performance Limit State Function. Multidimensional performance limit state function describes the condition that the structure will be in damage state when the multiple EDPs are considered. In the function, different performance limit states are viewed to be dependent, described by correlation coefficient (N_i) [24]:

$$L(R_1, \ldots, R_n) = \sum_{i=1}^{n}\left(\frac{R_i}{r_{\mathrm{lim},i}}\right)^{N_i} = 0, \tag{16}$$

where R_i is the EDP and $r_{\mathrm{lim},i}$ represents the corresponding thresholds of the demand parameters. When $L(R_1, \ldots, R_n) > 0$, the structure is in a specific damage state; when $L(R_1, \ldots, R_n) < 0$, the structure is in the safe state. Bidimensional and three-dimensional PLSs are shown in Figure 1 as an example.

In this study, the cumulative plastic strain (ε) and peak acceleration (Z) will be selected as the demand parameters for the structural and the nonstructural component, respectively. The bidimensional PLS function will be obtained:

$$\frac{Z_{\mathrm{LS}}}{Z_{\mathrm{LS0}}} + \left(\frac{\varepsilon_{\mathrm{LS}}}{\varepsilon_{\mathrm{LS0}}}\right)^N - 1 = 0, \tag{17}$$

where Z_{LS} and $\varepsilon_{\mathrm{LS}}$ are the maximum acceleration and cumulative plastic strain, respectively; Z_{LS0} and $\varepsilon_{\mathrm{LS0}}$ are the corresponding threshold values; and N represents the correlation coefficient.

After the PSDM and the PLS function are determined, multidimensional fragility can be calculated by multidimensional integration. The integral function is PSDM, and the failure domain is determined by PLS function.

5. Case Study

The case study structure is a 2-bay 2-story frame located in the structural laboratory at Georgia Tech for NEES (Network for Earthquake Engineering Simulation) project research (Figure 2), which aims to study the structural seismic performance under different reinforcement measures. The intermediate four frames are not connected with each other (Figure 3), and the outermost frames are used to prevent lateral collapse during the laboratory test. Buildings that were constructed before the 1970s can have significant deficiencies in their overall structural configuration and detailing. Because there was no seismic design guidance at that time, the seismic resistance against lateral loads for these structures does not usually meet current code requirements. The 2-bay 2-story frame in this study is just the structure before the 1970s. The utilized load and design codes are based on the *Structural Engineers Association of California (SEAOC) Blue Book*. Typical frame details in pre-1976 buildings are described as follows: generally, longitudinal reinforcement in beams was not continuous. Longitudinal reinforcement in columns was lap-spliced with short length. In addition, transverse reinforcement was not proportioned to prevent lap or shear failures, and details usually included open stirrups, wide spacing, and 90-degree bend hoops. Joint transverse reinforcement was uncommon. All these details can result in performance with inadequate lateral displacement ductility and inadequate protection against vertical collapse.

The finite element model (FEM) for the structure was established through SAP2000 (Figure 4). The seismic precautionary intensity is 7 degrees, and the design earthquake acceleration is 0.1 g. Elasticity modulus of concrete and steel bar are $E_c = 30$ GPa and $E_s = 200$ GPa, respectively. Poisson's ratio of concrete and steel bar are $\mu_c = 0.2$ and $\mu_s = 0.3$, respectively. The reinforced concrete density is 2500 kg/m^3. The plastic hinges are simulated at the ends of beams and columns. First-order resonance frequency is 1.733 Hz according to the modal analysis results. On the basis of those site and structural information, the earthquake influence coefficient curve will be calculated as the target response

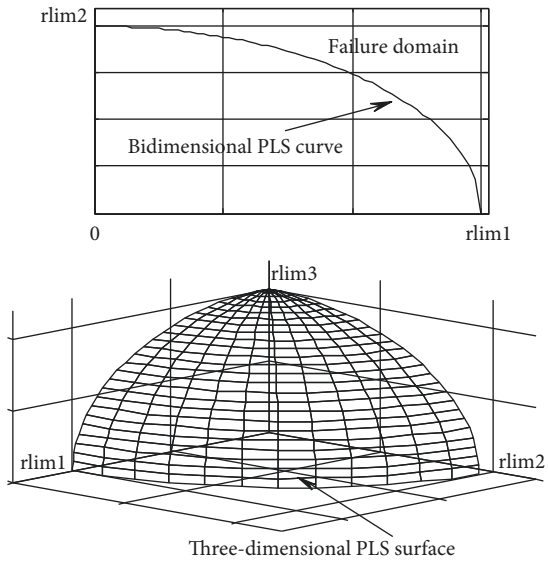

Figure 1: Bidimensional and three-dimensional PLSs. This figure is reproduced from [25] (under the Creative Commons Attribution License/public domain).

Figure 2: NEES frame structure. This figure is reproduced from [25] (under the Creative Commons Attribution License/public domain).

Figure 3: Four separate frames.

spectrum for earthquake records selection in PEER (Pacific Earthquake Engineering Earthquake Research Center) database. Finally, a set of 20 earthquake records, consistent with target response spectrum, are selected as the input for nonlinear dynamic time analysis, and they are provided in Table 1 with corresponding earthquake magnitude and epicentral distance.

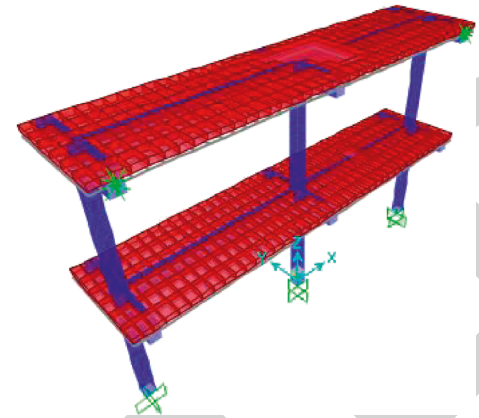

Figure 4: Three-dimensional FEM model. This figure is reproduced from [25] (under the Creative Commons Attribution License/public domain).

Table 1: Selected earthquake records.

Name	Magnitude	Epicentral distance (km)
FRIULI/FOC-NS	5.5	18.2
NORTHR/ORR090	6.7	22.6
NORTHR/BLD090	6.7	31.3
NORTHR/CHL070	6.7	23.7
NORTHR/PKC090	6.7	8.2
NORTHR/GLP177	6.7	25.4
NORTHR/LUC005	6.7	57.4
WHITTIER/A-SEC205	6	32.6
COYOTELK/G06230	5.7	3.6
CHICHI/NSY-E	7.6	9.7
CHICHI/CHY015-E	7.6	43.51
PARKF/C12050	6.1	14.7
WHITTIER/A-MAN090	6	28.9
KOBE/SHI000	6.9	15.5
KOBE/OSA000	6.9	8.5
KOBE/KAK000	6.9	26.4
NORTHR/BLF206	6.7	12.3
SUPERST/B-WLF225	6.7	27.1
IMPVALL/A-E03140	5.2	17.9
IMPVALL/H-E03140	6.5	9.3

5.1. Probability Distribution for Structural Responses. In this study, PGA is selected as the seismic intensity parameter. PGA is defined as the maximum ground acceleration of the ground motion, and it is a critical intensity measure for the earthquake. In addition, the design basis of earthquake ground motion is usually defined by PGA. Hence, PGA was chosen to characterize the seismic intensity level in this study. The selected 20 earthquake records are scaled to be different intensity levels, i.e., 0.05 g, 0.15 g, 0.35 g, 0.55 g, 0.75 g, and 0.95 g, as the input for nonlinear time-history analysis. Maximum structural responses including interstory drift and cumulative plastic strain are recorded (after the rotation angle and bending moment of the plastic hinge are obtained, cumulative plastic strain can be calculated according to equations (12) and (13)), with an assumption that their probability distributions obey the lognormal distribution, and the corresponding distribution parameters are estimated.

Table 2: Distribution parameters for maximum interstory drift.

Story	Parameters	PGA					
		0.05 g	0.15 g	0.35 g	0.55 g	0.75 g	0.95 g
1st story	μ_θ	−7.224	−6.165	−5.355	−4.925	−4.631	−4.408
	σ_θ	0.436	0.435	0.423	0.418	0.415	0.415
2nd story	μ_θ	−7.288	−6.221	−5.412	−4.979	−4.682	−4.456
	σ_θ	0.407	0.393	0.386	0.387	0.386	0.386

Tables 2 and 3 show the parameter estimation results for maximum interstory drift and CPS responses. μ and σ are the logarithmic mean and logarithmic standard deviation, respectively.

5.2. Determination of Cumulative Plastic Strain Thresholds. According to US FEMA 273, interstory drift thresholds for four PLS levels, i.e., normal operation (NO, no damage), immediate occupancy (IO), life safety (LS), and collapse prevention (CP), are 0.2%, 0.5%, 1.5%, and 2.5%, respectively. And the probability distribution of the maximum interstory drift is obtained (Table 2). Thus, the fragility curves of the structure on the basis of maximum interstory drift can be constructed. A series of cumulative plastic strain thresholds are assumed, and the corresponding fragility curves can be obtained. These two kinds of fragility curve are drawn in the same coordinate system, shown in Figure 5. The cumulative plastic strain thresholds will be determined by comparing the similarity between these two kinds of fragility curves.

Figure 5 shows that the fragility curves with cumulative plastic strain threshold values of 0.002, 0.004, 0.008, and 0.016 have a good consistence with four fragility curves corresponding NO, IO, LS, and CP. These values will be viewed as the thresholds for these four PLSs. The corresponding damage description is shown in Table 4. The fragility curves with cumulative plastic strain threshold value of 0.003 and 0.010 were also provided for the illustration. However, the fragility curves with cumulative plastic strain threshold value of 0.003 and 0.010 do not coincide with any curves based on interstory drift. Thus, these CPS values will not be adopted for the PLS threshold. The damage description for the four limit states is provided as follows: NO represents almost no damage for structural and nonstructural components; IO represents slight damage for structural and nonstructural components; LS represents certain damage for columns and beams and no danger for life safety; CP represents extensive damage with danger for life safety.

5.3. Multidimensional Fragility Analysis Based on CPS. The cumulative plastic strain and floor acceleration response are selected as quantitative performance parameters for the structural and nonstructural components, respectively. Multidimensional probabilistic seismic demand model can be obtained according to equation (15). On the basis of PLS threshold value, multidimensional performance limit state function can be constructed according to equation (17). Further, Monte Carlo will be employed to calculate the structural damage probability. Finally, cumulative distribution function of the lognormal distribution will be used for multidimensional fragility curve fitting. In addition, the sensitivity of fragility to acceleration threshold and PLS correlation will be investigated.

Table 3: Distribution parameters for maximum CPS.

PGA	0.05 g	0.15 g	0.35 g	0.55 g	0.75 g	0.95 g
μ_ε	−5.940	−5.382	−5.016	−4.807	−4.585	−4.338
$\sum_\varepsilon$	0.508	0.440	0.329	0.349	0.332	0.273

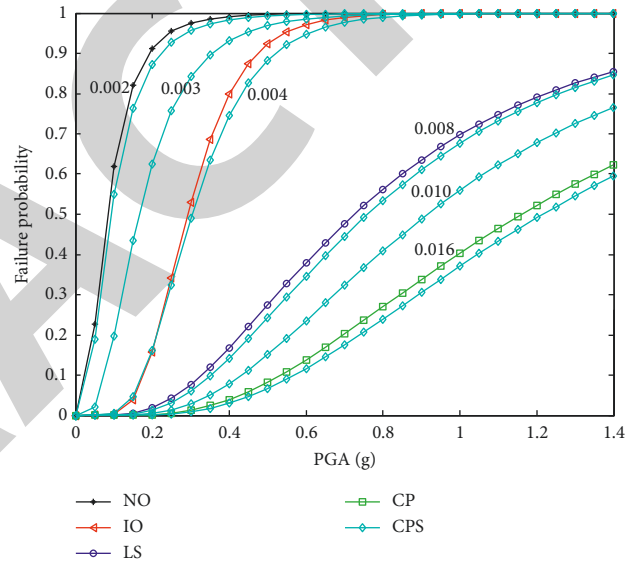

Figure 5: Comparison of two kinds of fragility curves. This figure is reproduced from [25] (under the Creative Commons Attribution License/public domain).

Table 4: CPS thresholds for different PLSs.

PLS	NO	IO	LS	CP
CPS threshold	0.002	0.004	0.008	0.016

Figure 6 shows the influence of acceleration threshold on the multidimensional fragility for the four PLSs, i.e., NO, IO, LS, and CP. The acceleration threshold is increased from 0.4 g to infinity, and the corresponding fragility curves are given. It is shown that with the increase of acceleration threshold, the failure probability decreases and the fragility curve moves down. When the acceleration threshold is infinity, the multidimensional fragility

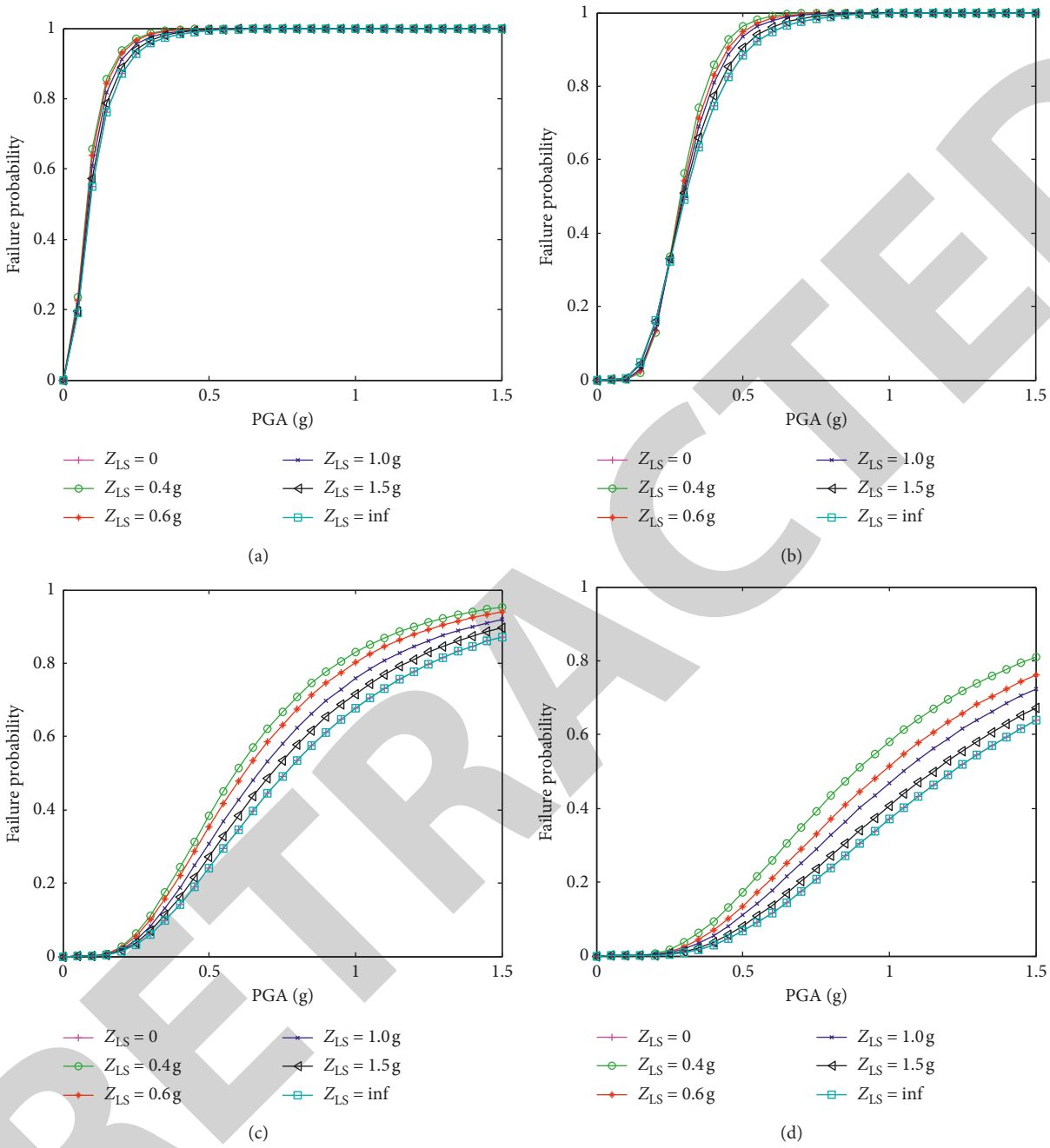

Figure 6: Sensitivity analysis of multidimensional fragility curves to acceleration threshold. (a) Normal operation PLS. (b) Immediate occupancy PLS. (c) Life safety PLS. (d) Collapse prevention PLS.

overlaps with fragility considering only the cumulative plastic strain.

The impact of acceleration threshold on fragility curves under NO and IO damage states is relatively small (when the threshold value changes, the fragility changes little). However, acceleration threshold has great influence on fragility curves under LS and CP damage states (when the threshold value changes, the fragility changes significantly). Thus, for these two kinds of limit states, choosing a reasonable acceleration threshold is essential for fragility assessment.

Correlation coefficient of engineering demand parameters is represented by ρ in the range from 0 to 1. When the correlation coefficient is set to 0, the engineering demand parameters are viewed to be unrelated. As the value increases, the correlation increases. Figure 7 shows the sensitivity of multidimensional fragility to the correlation coefficient of engineering demand parameters, i.e., CPS and acceleration. It can be seen that as the correlation coefficient increases, multidimensional fragility curves go down slightly for all performance levels. Overall, engineering demand

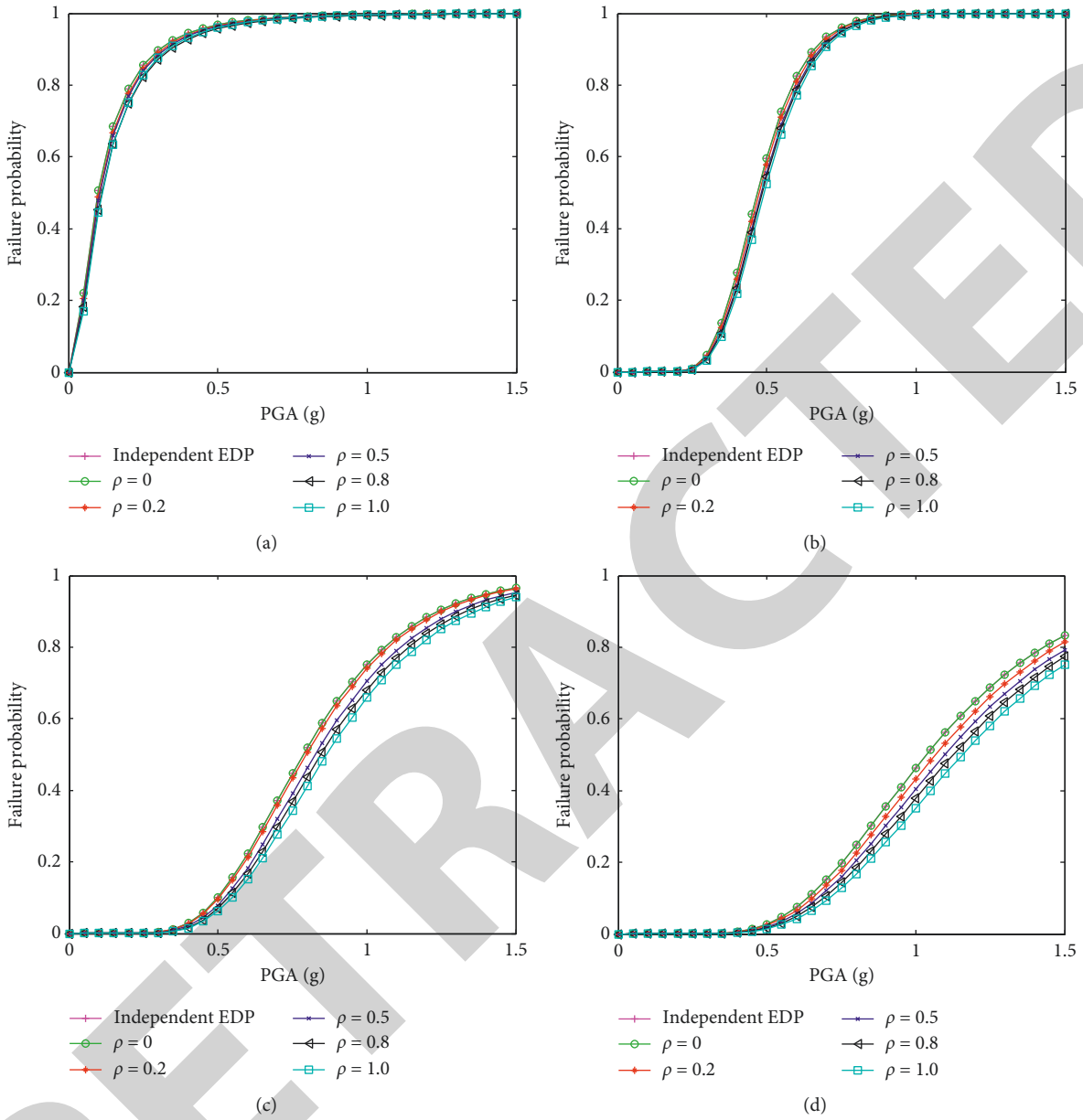

Figure 7: Sensitivity analysis of multidimensional fragility curves to EDP correlation. (a) Normal operation PLS. (b) Immediate occupancy PLS. (c) Life safety PLS. (d) Collapse prevention PLS.

parameter correlation does not affect the fragility as much as aforementioned PLS threshold.

Performance limit state correlation is described by the parameter N in equation (17). N ranges from 0 to infinity, and the correlation decreases with the increase of N. For instance, when $N = 1$, the two PLSs are linearly related. When N is infinite, the two limit states are independent with each other. Figure 8 shows the influence of PLS correlation on multidimensional fragility for four PLSs. It is shown that as the value of N increases, fragility curve goes down, especially for LS and CP performance levels. That is, when the PLS correlation is neglected, a lower failure probability will be obtained, resulting non-conservative estimation, which is adverse to the safety of engineering structures. Thus, the correlation between the performance limit states cannot be ignored for multidimensional fragility analysis.

6. Conclusions

(1) In this study, the cumulative plastic strain damage index is proposed on the basis of plastic dissipation energy, which is highly related with structural damage under earthquakes. It is concluded that this damage index can fully consider the damage accumulation effect under earthquakes, making up the deficiency of interstory drift damage index in this respect.

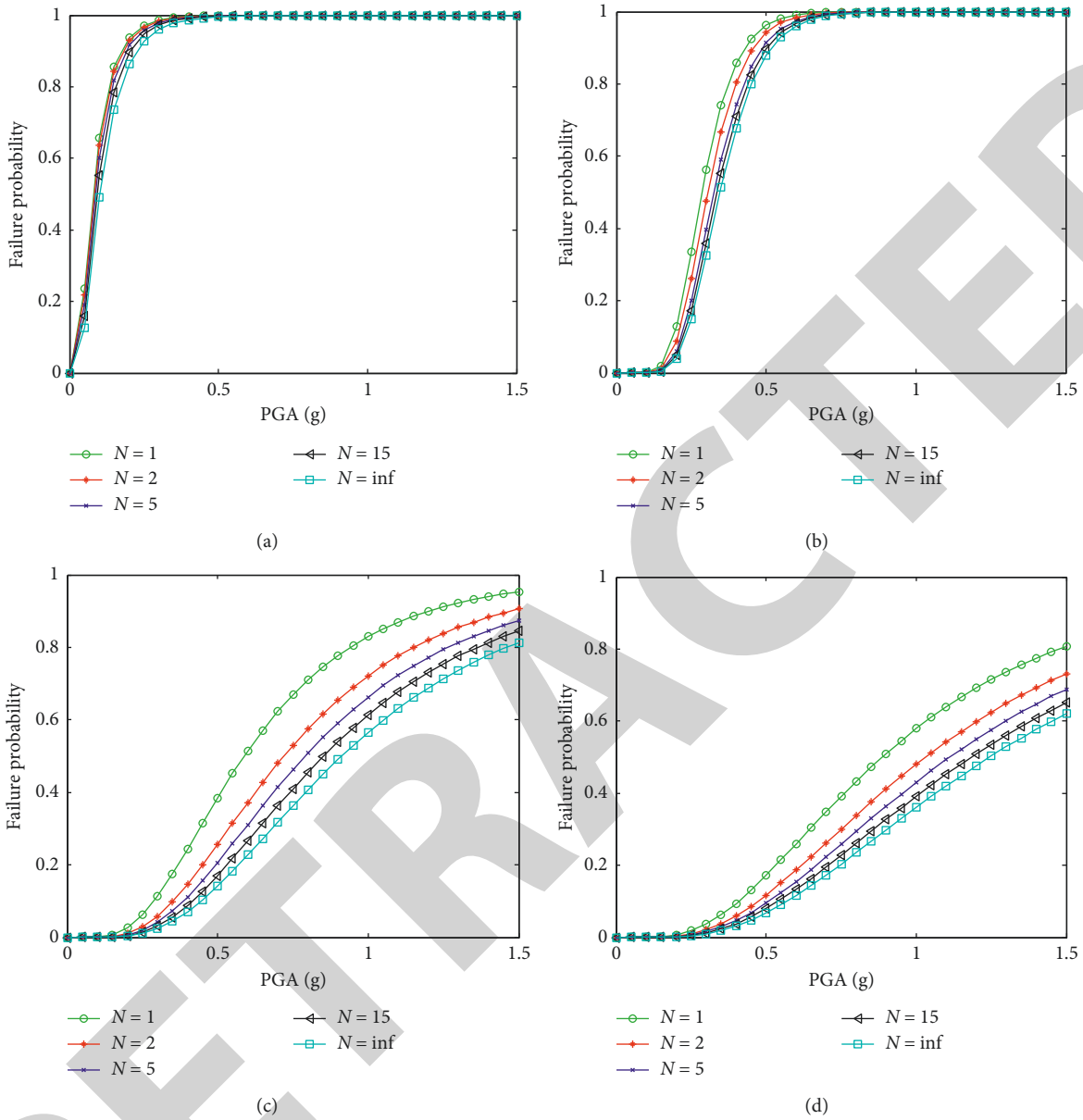

Figure 8: Sensitivity analysis of multidimensional fragility curves to PLS correlation. (a) Normal operation PLS. (b) Immediate occupancy PLS. (c) Life safety PLS. (d) Collapse prevention PLS.

(2) The cumulative plastic strain is integrated into the framework of multidimensional fragility, and a NEES frame structure is employed as a case study structure to illustrate the applicability of this method. CPS and the maximum floor acceleration are selected as the structural and nonstructural engineering demand parameters, respectively. On the basis of PLS threshold values, multidimensional PLS function can be developed. Through nonlinear time-history analysis, maximum structural responses can be obtained for the construction of multidimensional PSDM. Finally, the multidimensional fragility can be estimated by multiple integral.

(3) The influence of PLS threshold value on the multidimensional fragility is investigated. Multidimensional fragility for the NEES case study structure is sensitive to the PLS threshold. As acceleration threshold increases, the failure probability decreases and the fragility curve goes down. The impact of acceleration threshold on fragility curves under NO and IO damage states is relatively small. However, acceleration threshold has great influence on fragility curves under LS and CP damage states.

(4) The sensitivity of multidimensional fragility to EDP correlation and PLS correlation is also investigated. Performance limit state correlation has great influence on multidimensional fragility. It is shown that as the PLS correlation weakens, fragility decreases, especially for LS and CP damage states. That is, a lower failure probability, i.e.,

nonconservative estimation, will be obtained, which is adverse to the safety of engineering structures. In addition, it is indicated with the increase of the correlation coefficient, multidimensional fragility curves go down slightly for all performance levels. Thus, EDP correlation does not affect the fragility as much as PLS threshold and PLS correlation.

Notations

n: Number of horizontal degrees of freedom
m: Number of rotational degrees of freedom
$X(t)$: Displacement vector
$X'(t)$: Elastic displacement vector
$X''(t)$: Plastic displacement
$M'(t)$: Elastic moment vector corresponding to the elastic displacement
$M''(t)$: Plastic moment vector corresponding to the plastic displacement
K: Overall stiffness matrix
K': Transformation matrix between the rotation angle and the restoring force
K'': Transformation matrix between the rotation angle and the restoring bending moment
M: Mass matrix
C: Damping matrix
$\ddot{x}(t)$: Acceleration of the structure relative to the ground
$\dot{x}(t)$: Relative speed
$\ddot{g}(t)$: Acceleration of the ground
$y(t)$: Absolute displacement
PE_i: Plastic dissipation energy at the ith plastic hinge
ε: Cumulative plastic strain
f_y: Yield stress of the component
A_i: Sectional area of the component
d_i: Length of the component
Ri: Seismic demand parameters
$r_{\lim,i}$: Performance limit state threshold
I: Ground motion intensity parameter
μ: Mean vector
$\sum$: Covariance matrix
N_i: Correlation coefficient
$L(R_1, \ldots, R_n)$: Limit state function
R_i: EDP
$r_{\lim,i}$: Corresponding thresholds of the demand parameters
Z: Peak acceleration
Z_{LS}: Maximum acceleration
ε_{LS}: Maximum
Z_{LS0}: Acceleration threshold value
ε_{LS0}: Cumulative plastic strain threshold value.

Data Availability

The data used to support the findings of this study are available from the corresponding author upon request.

Conflicts of Interest

The authors declare that they have no conflicts of interest.

Acknowledgments

The study was supported by the Fundamental Research Funds for the Central Universities under Award Number 2019QNA20. The authors wish to express their gratitude to staff and students in the Structural Engineering Laboratory for their extensive assistance. The data used to support the findings of this study are available from the corresponding author upon request.

References

[1] Y. Hose, P. Silva, and F. Seible, "Development of a performance evaluation database for concrete bridge components and systems under simulated seismic loads," *Earthquake Spectra*, vol. 16, no. 2, pp. 413–442, 2000.

[2] S. Mahboubi and M. R. Shiravand, "Proposed input energy-based damage index for RC bridge piers," *Journal of Bridge Engineering*, vol. 24, no. 1, article 04018103, 2018.

[3] E. Bojórquez, V. Baca, J. Bojórquez, A. Reyes-Salazar, R. Reyes-Salazar, and M. Barraza, "A simplified procedure to estimate peak drift demands for mid-rise steel and R/C frames under narrow-band motions in terms of the spectral-shape-based intensity measure I," *Engineering Structures*, vol. 150, pp. 334–345, 2017.

[4] E. Farsangi, A. Tasnimi, T. Yang et al., "Seismic performance of a resilient low-damage base isolation system under combined vertical and horizontal excitations," *Smart Structures and Systems*, vol. 22, no. 4, pp. 383–397, 2018.

[5] P. Xiang, A. Nishitani, S. Marutani et al., "Identification of yield drift deformations and evaluation of the degree of damage through the direct sensing of drift displacements," *Earthquake Engineering & Structural Dynamics*, vol. 45, no. 13, pp. 2085–2102, 2016.

[6] H. Kazemi, M. Ghafory-Ashtiany, and A. Azarbakht, "Development of fragility curves by incorporating new spectral shape indicators and a weighted damage index: case study of steel braced frames in the city of Mashhad, Iran," *Earthquake Engineering and Engineering Vibration*, vol. 16, no. 2, pp. 383–395, 2017.

[7] D. Lv and G. Wang, "Decision-making method of optimal fortification level for seismic structures based on damage performance," *China Civil Engineering Journal*, vol. 34, no. 1, pp. 44–49, 2001.

[8] Y. Ding, F. Guo, and Z. Li, "Elasto-plastic analysis of spatial trusses under earthquake excitations considering damage accumulation effect," *Engineering Mechanics*, vol. 22, no. 1, pp. 54–58, 2005.

[9] H. Naderpour and M. Mirrashid, "Shear failure capacity prediction of concrete beam–column joints in terms of ANFIS and GMDH," *Practice Periodical on Structural Design and Construction*, vol. 24, no. 2, article 04019006, 2019.

[10] S. M. Khatami, H. Naderpour, R. C. Barros, and R. Jankowski, "Verification of formulas for periods of adjacent buildings used to assess minimum separation gap preventing structural pounding during earthquakes," *Advances in Civil Engineering*, vol. 2019, Article ID 9714939, 8 pages, 2019.

[11] R. Park, "Ductile design approach for reinforced concrete frames," *Earthquake Spectra*, vol. 2, no. 3, pp. 565–619, 1986.

[12] A. S. Whittaker and E. Elsesser, "Seismic design criteria for transportation structures," in *US Conference on Lifeline Earthquake Engineering*, San Francisco, CA, USA, August 1991.

[13] G. H. Powell and R. Allahabadi, "Seismic damage prediction by deterministic methods: concepts and procedures," *Earthquake Engineering & Structural Dynamics*, vol. 16, no. 5, pp. 719–734, 1988.

[14] A. Bassam, A. Iranmanesh, and F. Ansari, "A simple quantitative approach for post earthquake damage assessment of flexure dominant reinforced concrete bridges," *Engineering Structures*, vol. 33, no. 12, pp. 3218–3225, 2011.

[15] Y. J. Park and A. H. S. Ang, "Mechanistic seismic damage model for reinforced concrete," *Journal of Structural Engineering*, vol. 111, no. 4, pp. 722–739, 1985.

[16] A. Teran-Gilmore, A. Sanchez-Badillo, and M. Espinosa-Johnson, "Performance-based seismic design of reinforced concrete ductile buildings subjected to large energy demands," *Earthquakes and Structures*, vol. 1, no. 1, pp. 69–91, 2010.

[17] S. A. Diaz, L. G. Pujades, A. H. Barbat, Y. F. Vargas, and D. A. Hidalgo-Leiva, "Energy damage index based on capacity and response spectra," *Engineering Structures*, vol. 152, pp. 424–436, 2017.

[18] A. Belejo, A. R. Barbosa, and R. Bento, "Influence of ground motion duration on damage index-based fragility assessment of a plan-asymmetric non-ductile reinforced concrete building," *Engineering Structures*, vol. 151, pp. 682–703, 2017.

[19] A. Khaloo, S. Nozhati, H. Masoomi, and H. Faghihmaleki, "Influence of earthquake record truncation on fragility curves of RC frames with different damage indices," *Journal of Building Engineering*, vol. 7, pp. 23–30, 2016.

[20] K. K. F. Faghihmaleki and R. Yang, "Inelastic dynamic response of structures using force analogy method," *Journal of Engineering Mechanics*, vol. 125, no. 10, pp. 1190–1199, 1999.

[21] H. Naderpour and S. M. Khatami, "A new model for calculating the impact force and the energy dissipation based on CR-factor and impact velocity," *Scientia Iranica*, vol. 22, no. 1, pp. 59–68, 2015.

[22] S.-H. Oh and S.-H. Shin, "A proposal for a seismic design process for a passive control structural system based on the energy equilibrium equation," *International Journal of Steel Structures*, vol. 17, no. 4, pp. 1285–1316, 2017.

[23] Q. A. Wang, Z. Wu, and S. Liu, "Multivariate probabilistic seismic demand model for the bridge multidimensional fragility analysis," *KSCE Journal of Civil Engineering*, vol. 22, no. 9, pp. 3443–3451, 2018.

[24] G. Cimellaro and A. Reinhorn, "Multidimensional performance limit state for hazard fragility functions," *Journal of Engineering Mechanics*, vol. 137, no. 1, pp. 47–60, 2010.

[25] Q. A. Wang, Z. Y. Wu, and Y. Wang, "Multi-dimensional fragility analysis considering structural cumulative plastic dissipation energy and its application to a NEES frame structure," in *Proceedings of the 13th International Conference on Applications of Statistics and Probability in Civil Engineering (ICASP13)*, Seoul, South Korea, May 2019.